# Motion Planning with Precedence Specifications via Augmented Graphs of Convex Sets

Shilin You, Gael Luna, Juned Shaikh, David Gostin, Yu Xiang, Justin Koeln, Tyler Summers

Abstract—We present an algorithm for planning trajectories that avoid obstacles and satisfy key-door precedence specifications expressed with a fragment of signal temporal logic. Our method includes a novel exact convex partitioning of the obstacle free space that encodes connectivity among convex free space sets, key sets, and door sets. We then construct an augmented graph of convex sets that exactly encodes the key-door precedence specifications. By solving a shortest path problem in this augmented graph of convex sets, our pipeline provides an exact solution up to a finite parameterization of the trajectory. To illustrate the effectiveness of our approach, we present a method to generate key-door mazes that provide challenging problem instances, and we perform numerical experiments to evaluate the proposed pipeline. Our pipeline is faster by several orders of magnitude than recent state-ofthe art methods that use general purpose temporal logic tools.

### I. Introduction

Motion planning is a fundamental problem in robotics and autonomous systems involving the computation of feasible trajectories for agents navigating through complex environments with various constraints [1], [2]. Many approaches have been developed over several decades, including sampling-based methods, combinatorial graph search, and optimization-based techniques. Due to inherent complexities in motion planning, these approaches must navigate trade-offs between computational efficiency, optimality, and the ability to handle rich geometric, dynamic, and logical constraints.

Recent research has developed a promising new framework involving shortest path problems in graphs of convex sets (GCS) [3], [4]. This approach elegantly integrates the combinatorial and continuous features whose combination is part of what make motion planning challenging. The combinatorial structure of a graph encodes discrete components, such as region transitions, logical constraints, or contact modes, while each node and edge of the graph is associated with convex sets and functions that describe the continuous spatiotemporal geometry of the problem. This enables powerful tools from convex optimization and mixed-integer optimization that can compute globally optimal or certifiably near-optimal solutions for complex environments and constraints.

We formulate a motion planning problem with precedence specifications and present a solution method based on graphs

The authors are with the Department of Mechanical Engineering at University of Texas at Dallas. Email: tyler.summers@utdallas.edu

of convex sets. The GCS framework is particularly well-suited to problems with logical precedence constraints that can be encoded with temporal logic (TL). In particular, we consider a class of environments consisting of obstacles, keys, and doors, where keys can be used to unlock doors to open potentially shorter paths to a terminal goal state. The objective is to find an optimal path from an initial state to a goal state, accounting for keys being able to unlock doors, which may be required to find an optimal path. An overview of the proposed approach is shown in Fig. 1.

Our main contributions are:

- We develop an exact convex partitioning of the free space, key, and door sets, which also produces a labeled graph describing connectivity among the free space, key, and door sets (Section III, Algorithm 1).
- We develop an algorithm to construct an augmented graph of convex sets that exactly encodes key-door precedence logic (Section IV, Algorithm 2). An exact solution (up to trajectory parameterization) to the motion planning problem with precedence constraints is then obtained by solving a shortest path problem on this augmented graph of convex sets.
- We present a method to generate key-door maze environments and perform numerical experiments to evaluate the performance of the proposed methods. Our results also include instances from [5], where our methods are faster by several orders of magnitude, and a collection of maze environments created with our maze generator. We study the optimality gap and show that on all instances, the solution obtained with our method is within 1% of the optimal value, and in many cases is globally optimal. Our code will be provided in an open-source repository.

Motion planning with general temporal logic constraints using the GCS framework has been recently studied in [5]. Our key insight is that by restricting attention to a specific fragment of temporal logic specifications involving key-door precedence logic and exploiting this structure to build an augmented graph of convex sets that encodes this logic, we achieve several orders of magnitude speed-up over general purpose temporal logic tools (which to our best knowledge represents the state-of-the-art). This "bottom-up" approach focuses on specific TL fragments with exploitable structure rather than "top-down" approaches that aim to handle arbitrary TL specifications built from a given grammar. Our approach can be adapted to additional temporal logic

fragments that can capture a wide variety of practical motion and task planning problems.

### Related Work

The main inspirations of the work are [4], [3], [5]. Our problem can also be considered as a type of task and motion planning problem combining geometric and logical components [6].

### II. PROBLEM FORMULATION

Consider a robot operating in a bounded environment  $\mathcal{X} \subset \mathbf{R}^d$ . The environment contains a set of obstacles  $\mathcal{O} = \{\mathcal{O}_i\}_{i=1,\dots,n_O}$  with  $\mathcal{O}_i \subset \mathcal{X}$ . The obstacle-free space is denoted by  $\mathcal{C} = \mathcal{X} - \mathcal{O}$ . The environment also contains a set of doors  $\mathcal{D} = \{\mathcal{D}_i\}_{i=1,\dots,n_D}$ , which are obstacles that can be "unlocked" and removed from the environment using a corresponding set of keys  $\mathcal{K} = \{\mathcal{K}_i\}_{i=1,\dots,n_K}$ . The environment and all obstacle, key, and door sets are assumed to be polytopes with given half-space representation:

$$\mathcal{X} = \{x \in \mathbf{R}^d \mid H_X x \leq g_X\}$$

$$\mathcal{O}_i = \{x \in \mathbf{R}^d \mid H_{O_i} x \leq g_{O_i}\}$$

$$\mathcal{D}_i = \{x \in \mathbf{R}^d \mid H_{D_i} x \leq g_{D_i}\}$$

$$\mathcal{K}_i = \{x \in \mathbf{R}^d \mid H_{K_i} x \leq g_{K_i}\}.$$

We assume that the number of keys is equal to the number of doors  $(n = n_K = n_D)$ , and that each key is uniquely associated with a door. Without loss of generality, we assume key i unlocks door i for  $i = 1, ..., n_K$ . The key-door logic can be expressed by a mapping  $\mathbf{D} : 2^K \to 2^D$ , which specifies the set of doors that are unlocked by a given set of keys. In our setting, this is simply the identity mapping.

Our goal is to find a trajectory q over a time horizon T that solves the following optimization problem:

The objective is a weighted sum of the trajectory length and the time horizon with weights  $\alpha$  and  $\beta$ , respectively. The first constraint requires the trajectory to be in the union of free space sets, key sets, and door sets for all time. The second constraint is a temporal logic specification that enforces the key-door precedence logic to be satisfied. The third constraint requires the velocity to be in the convex set  $\mathcal Q$  for all time. The remaining constraints specify initial and terminal conditions for the position and velocity.

The optimization problem (1) is infinite-dimensional, so candidate trajectories can be parameterized with piecewise Bézier curves defined by a finite set of control points. It is straightforward to include additional objective function

terms and constraints that are convex in this parameterization. For example, penalties and constraints on higher-order derivatives promote additional smoothness on the trajectory q. Ensuring that the trajectory is differentiable a certain number of times facilitates the design of dynamically feasible trajectories for fully actuated and differentially flat systems.

### A. Precedence Constraints via Signal Temporal Logic

We use signal temporal logic (STL) [7] to encode the key-door precedence specifications. STL is a variation of temporal logic [8] that offers a general and powerful framework to specify complex spatiotemporal tasks and constraints. A STL formula can be composed from the following grammar

$$\varphi ::= \top \mid p \mid \neg \varphi \mid \varphi_1 \land \varphi_2 \mid \varphi_1 \lor \varphi_2 \mid \varphi_1 \mathcal{U} \varphi_2 \mid \varphi_1 \mathcal{R} \varphi_2,$$
 (2)

by starting from a set of atomic propositions AP with  $p \in AP$  and recursively applying boolean operators:  $\neg$  (not),  $\wedge$  (and), and  $\vee$  (or), and temporal operators:  $\mathcal{U}$  (until), and  $\mathcal{R}$  (release). The until operator  $\phi \mathcal{U} \psi$  is satisfied if  $\phi$  remains true until  $\psi$  becomes true. The release operator  $\phi \mathcal{R} \psi$  is satisfied if  $\psi$  remains true until and including when  $\phi$  becomes true, and if  $\phi$  never becomes true, then  $\psi$  always remains true; in other words,  $\phi$  releases  $\psi$ . Additional temporal operators can be defined, such as eventually  $(\mathcal{F}\varphi := \neg \mathcal{U}\varphi)$  and always  $(G\varphi := \neg \mathcal{F} \neg \varphi)$ . STL operators and formulas can also be restricted to hold over specific and finite time intervals.

The key-door precedence logic can be expressed using the release operator. In particular, we utilize a specific fragment of STL of the form:

$$\varphi = (\mathcal{K}_1 \,\mathcal{R} \,\neg \mathcal{D}_1) \wedge (\mathcal{K}_2 \,\mathcal{R} \,\neg \mathcal{D}_2) \wedge \cdots \wedge (\mathcal{K}_n \,\mathcal{R} \,\neg \mathcal{D}_n) \wedge \mathcal{F}(\mathcal{T}),$$

which releases the door constraint when the corresponding key set is entered and requires the terminal condition  $\mathcal{T}$  to eventually be reached. Note that this formulation makes picking up the keys optional, unless doing so is required to reach the target. Alternatively, key-door logic that requires keys to be picked up regardless of whether they are needed can be expressed with the until operator:

$$\varphi = (\neg \mathcal{D}_1 \mathcal{U} \mathcal{K}_1) \wedge (\neg \mathcal{D}_2 \mathcal{U} \mathcal{K}_2) \wedge \cdots \wedge (\neg \mathcal{D}_n \mathcal{U} \mathcal{K}_n) \wedge \mathcal{F}(\mathcal{T}),$$

which prevents passage through the door sets until the corresponding key sets are entered. When the environment and obstacles impose the requirement to pick up the keys in order to reach the target, these specifications are equivalent.

### B. Graphs of Convex Sets

The graph of convex sets (GCS) framework [3] consists of a graph  $\mathcal{G}(\mathcal{V},\mathcal{E})$  with vertices  $\mathcal{V}$  and edges  $\mathcal{E}$ . Each vertex  $v \in \mathcal{V}$  is associated with a convex set  $\mathcal{X}_v$  and a variable  $x_v \in \mathcal{X}_v$ . For an edge  $e = (u,v) \in \mathcal{E}$ , its length is given by a nonnegative, convex, and proper function of the corresponding vertex variables  $\ell_e(x_u,x_v)$ . An edge can optionally also be associated with a constraint  $(x_u,x_v) \in \mathcal{X}_e$ ; this can be equivalently included by allowing the length function to be extended-valued.

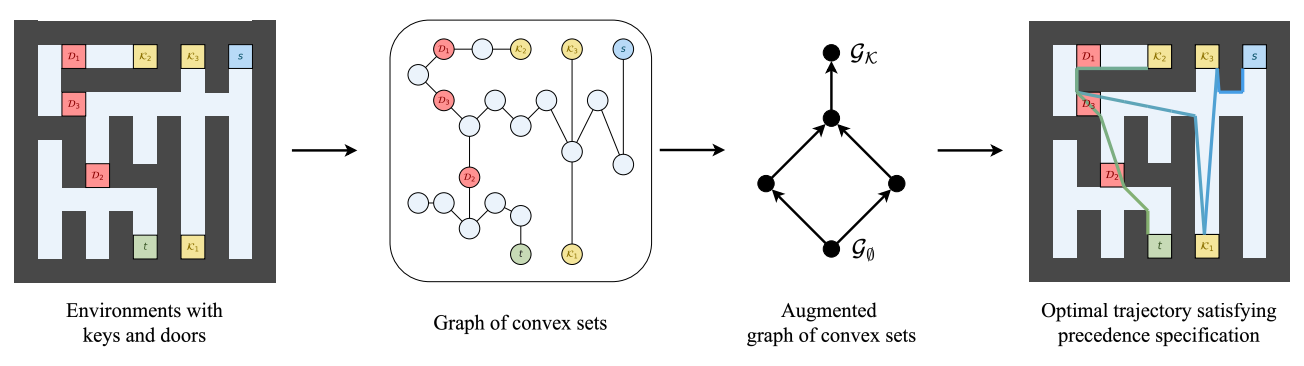


Fig. 1: Overview of the proposed approach. The environment is first partitioned and represented as a Graph of Convex Sets (GCS). An augmented GCS is then constructed to encode precedence specifications, and a shortest path problem is solved for the augmented GCS.

For a given start vertex  $s \in \mathcal{V}$  and target vertex  $t \in \mathcal{V}$ , a path p is a sequence of distinct vertices that connects s to t via an edge subset  $\mathcal{E}_p \subset \mathcal{E}$ . Denoting by  $\mathcal{P}$  the set of all paths from s to t in the graph  $\mathcal{G}$ , the shortest path problem in GCS is stated as

This problem seeks to simultaneously find a (discrete) path in the graph from the start vertex to the target vertex and the (continuous) values  $x_v$  for each vertex that minimize the total edge length across all edges in the path. Although this problem is computationally difficult in general, a novel and tight mixed-integer formulation was developed in [3]. This formulation uses a network flow formulation of the shortest path problem and exploits duality between perspective cones and valid inequality cones to convexify bilinear constraints that arise from the continuous vertex variables.

Further, a translation from the motion planning problem (without precedence constraints) into a shortest path problem in graphs of convex sets was developed in [4]. It was also observed that solving a convex relaxation of the mixed-integer formulation of (3) (by simply dropping binary constraints) and utilizing a cheap rounding algorithm allowed certifiably near-optimal or even optimal solutions for many practical motion planning problems. We refer readers to [3], [4] for many important details about reformulations.

Following the approaches of [4], [5], we will develop a pipeline to transform our problem (1) into a shortest path problem in a graph of convex sets [3]. First, we develop an exact convex partition of the obstacle-free space into a union of convex sets and construct a graph that encodes connectivity among free space, key, and door sets. Then, we propose a method to build an augmented graph of convex sets that encodes the key-door precedence logic. We demonstrate that a shortest path in this augmented graph of convex sets exactly solves our problem (1).

### III. EXACT CONVEX PARTITIONING OF THE FREE SPACE, KEY, AND DOOR SETS

This section presents an exact partitioning algorithm to represent the free space  $\mathcal{C}=\mathcal{X}-(\mathcal{O}\cup\mathcal{D}\cup\mathcal{K})$  as a union of convex sets of the form  $\mathcal{C}=\{\mathcal{C}_i\}_{i=1,\dots,n_C}$ , where the convex free space sets  $\mathcal{C}_i\subset\mathcal{X}$  intersect only at boundaries. Based on this partition, we construct a labeled graph  $\mathcal{G}(\mathcal{V},\mathcal{E})$ , where the vertices  $\mathcal{V}=\{\mathcal{V}_{\mathcal{C}},\mathcal{V}_{\mathcal{D}},\mathcal{V}_{\mathcal{K}}\}$  are labeled as either free space, key, or door sets, and an edge  $(u,v)\in\mathcal{E}$  connects vertices u and v if their corresponding convex sets share a facet.

### A. Cell Enumeration for Hyperplane Arrangements

We first collect all distinct hyperplanes that form the boundaries for the environment  $\mathcal{X}$ , obstacles  $\mathcal{O}$ , keys  $\mathcal{K}$ , and doors  $\mathcal{D}$  into a set  $\mathcal{H} = \{(h_i,g_i)\}_{i=1}^{n_h}$ , called a *hyperplane arrangement*. Let  $\mathcal{S}: \mathcal{X} \to \{+,-\}^{n_h}$  denote the sign function defined by

$$S(x) = \begin{cases} - & h_i^\top x \le g_i \\ + & h_i^\top x \ge g_i \end{cases} \quad \text{for } i = \{1, ..., n_h\}.$$

This function assigns to each point in  $\mathcal{X}$  a sign pattern, called a *marking*, that encodes which side of each hyperplane that point lies. For a fixed marking m, the set

$$\mathcal{P}_m = \{ x \in \mathcal{X} \mid \mathcal{S}(x) = m \}$$

is a (convex) polytope, referred to as a *cell* of the hyperplane arrangement. These sets form an exact convex partition of the environment  $\mathcal{X}$ , including a partition of the free space and the obstacle, key, and door sets.

To create a labeled graph of convex sets that captures all free space, key, and door sets, we must enumerate all nonempty cells of the hyperplane arrangement. The reverse search algorithm [9] can be used to enumerate all cells and their corresponding markings by solving a sequence of linear programs that effectively execute a depth-first search to construct a spanning tree of the cells. More recently, a method that exploits relationships between hybrid zonotopes and ReLU neural networks was proposed in [10].

Let  $M(\mathcal{X})$  denote the image of the sign function on the set  $\mathcal{X}$ , i.e., the set of all markings that define nonempty cells.

Although there are  $2^{n_h}$  possible markings, only a subset of them define nonempty cells. In fact, for  $n_h$  hyperplanes in d-dimensional space, Buck demonstrated the bound

$$|M(\mathbf{R}^d)| \le \sum_{i=0}^d \binom{n_h}{i} = O(n_h^d),$$

with the bound attained when the hyperplanes are in *general* position (no pair of hyperplanes is parallel and no point lies on more than d hyperplanes).

### B. Forming a Graph of Convex Sets from the Cell Enumeration

By associating a vertex with each cell, we define the vertex set  $\mathcal{V}$  for a graph of convex sets. The corresponding edge set can be determined by exploiting an important property of partitions based on hyperplane arrangements and markings. In particular, two cells share a facet if and only if their markings differ in only a single element. Therefore, for two cells  $\mathcal{P}_{m_1}$  and  $\mathcal{P}_{m_2}$ , there is an edge connecting them if  $\|m_1 - m_2\| = 2$ . Performing this comparison for each pair of cells generates the edge set  $\mathcal{E}$ .

It is easy to distinguish and label cells and vertices associated with key and door sets using the markings. For example, let  $H \subset \mathcal{H}$  be the subset of hyperplanes that define the boundary of any key or door. Then set of markings with a- in the corresponding entries, namely

$$M_H = \{ m \in M(\mathcal{X}) \mid m_i = - \quad \forall i \in H \}$$

correspond to cells whose union reconstructs that key or door set. In the graph, we merge all vertices associated with this set of markings. Performing this operation for each key and door generates the labeled vertex sets  $\mathcal{V}_{\mathcal{K}}$  and  $\mathcal{V}_{\mathcal{D}}$ . Similarly, all cells and corresponding nodes associated with obstacle cells can be identified and removed from the graph. The remaining vertices correspond to free space and define  $\mathcal{V}_{\mathcal{C}}$ .

Thus, we have constructed a labeled graph of convex sets  $\mathcal{G}(\mathcal{V},\mathcal{E})$  with  $\mathcal{V}=\{\mathcal{V}_{\mathcal{C}},\mathcal{V}_{\mathcal{K}},\mathcal{V}_{\mathcal{D}}\}$ , where the polytopes corresponding to  $\mathcal{V}_{\mathcal{C}}$  form an exact convex partition of the free space, and the edge set encodes connectivity among free space, key, and door sets that share a facet.

### C. Merging Free Space Cells to Reduce Graph Size

Although the graph from the previous section can immediately be used within the GCS motion planning framework, it may contain a large number of free space nodes, depending on the number of obstacles, keys, and doors, and especially the dimension d. The optimal complexity reduction problem is to find a *minimal* partition of the free space. This problem was studied in [11], where a branch-and-bound algorithm was developed to obtain a partition with a minimal number of polytopes by merging cells that preserve convexity. Alternatively, greedy algorithms can be used to quickly reduce the number of polytopes without necessarily obtaining a minimal partition [11], [10]. Our algorithm for exact convex partitioning and labeled GCS construction is summarized in Algorithm 1.

## **Algorithm 1:** Exact Convex Partition & Labeled GCS Construction

**Input:** Environment  $\mathcal{X}$ , obstacles  $\mathcal{O} = \{\mathcal{O}_i\}_{i=1,\dots,n_O}$ , keys,  $\mathcal{K} = \{\mathcal{O}_i\}_{i=1,\dots,n}$ , doors  $\mathcal{D} = \{\mathcal{D}_i\}_{i=1,\dots,n}$  all given in half-space representation

**Output:** Labeled graph of convex sets  $\mathcal{G}(\mathcal{V}, \mathcal{E})$  with  $\mathcal{V} = \{\mathcal{V}_{\mathcal{C}}, \mathcal{V}_{\mathcal{K}}, \mathcal{V}_{\mathcal{D}}\}$  and exact convex partition  $\mathcal{X} - \mathcal{O} \cup \mathcal{K} \cup \mathcal{D} = \{\mathcal{C}_i\}_{i=1}^{n_C}$ 

- 1: Form hyperplane arrangement from all boundaries
- 2: Enumerate cells in environment and generate markings  $M(\mathcal{X})$  (via reverse search or hybrid zonotopes)
- 3: Define vertex for each cell to form initial vertex set  $\mathcal V$
- 4: Define edge set  $\mathcal{E}$  between vertices whose markings differ in exactly one entry
- 5: for  $K_i \in K$ ,  $D_i \in D$  do
- 6: Merge and label corresponding cells and vertices
- 7: end for
- 8: for  $\mathcal{O}_i \in \mathcal{O}$  do
- 9: Merge and discard corresponding cells and vertices
- 10: **end for**
- 11: Merge free space nodes that preserve convexity (via optimal complexity reduction or greedy algorithm)
- 12: **return**  $\mathcal{G}(\mathcal{V}, \mathcal{E})$  with  $\mathcal{V} = {\mathcal{V}_{\mathcal{C}}, \mathcal{V}_{\mathcal{K}}, \mathcal{V}_{\mathcal{D}}}$

### IV. CONSTRUCTION OF AN AUGMENTED GRAPH OF CONVEX SETS ENCODING PRECEDENCE LOGIC

In this section, we describe how to construct an augmented graph of convex sets that encodes the key-door precedence constraints based on the labeled GCS  $\mathcal{G}(\mathcal{V},\mathcal{E})$  from Section III. The augmented GCS consists of copies of  $\mathcal{G}(\mathcal{V},\mathcal{E})$ , with different edge sets according to the current set of collected keys. By construction, every path connecting the starting node and a target node copy in the augmented GCS satisfies the key-door precedence constraints.

### A. Constructing the Augmented GCS

The augmented GCS is built recursively from the labeled graph  $\mathcal{G}(\mathcal{V},\mathcal{E})$  with  $\mathcal{V}=\{\mathcal{V}_{\mathcal{C}},\mathcal{V}_{\mathcal{D}},\mathcal{V}_{\mathcal{K}}\}$  based on a start node  $s\in\mathcal{V}_{\mathcal{C}}$  whose corresponding set contains the initial condition. The augmented GCS consists of  $n_K+1$  layers, where each layer represents reachable key subsets of a certain cardinality.

A simple 2-key environment is shown in Fig. 2, and the associated augmented GCS is shown in Fig. 3. We will refer to this as a running example throughout our description.

The Base Layer. The base layer of the augmented GCS corresponds to the empty key set  $\emptyset \in 2^{\mathcal{K}}$ . We define the base graph  $\mathcal{G}_{\emptyset}(\mathcal{V}_{\emptyset}, \mathcal{E}_{\emptyset})$ . The vertex set  $\mathcal{V}_{\emptyset}$  consists of a copy of all vertices in  $\mathcal{V}$ . The edge set is

$$\mathcal{E}_{\emptyset} = \mathcal{E} - \{(u, v) \in \mathcal{E} \mid u \in \mathcal{V}_{\mathcal{D}} \text{ or } v \in \mathcal{V}_{\mathcal{D}}\},$$

corresponding to the original edge set with all edges adjacent to door nodes removed. The base layer for the simple 2-key environment is shown at the bottom of Fig. 3.

Layer 1. The next layer of the augmented GCS corresponds to 1-element key sets that are reachable from the

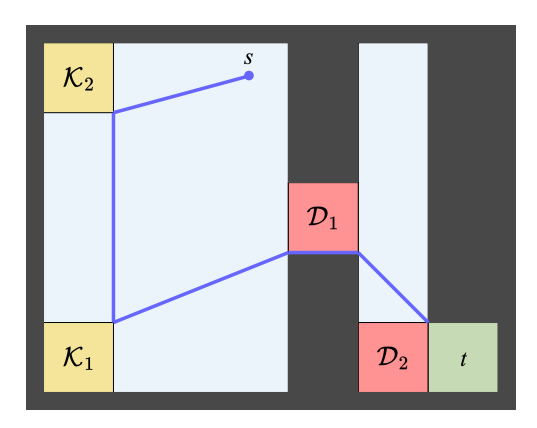


Fig. 2: A key-door environment with 2 keys and 2 doors. The blue line shows the optimal solution.

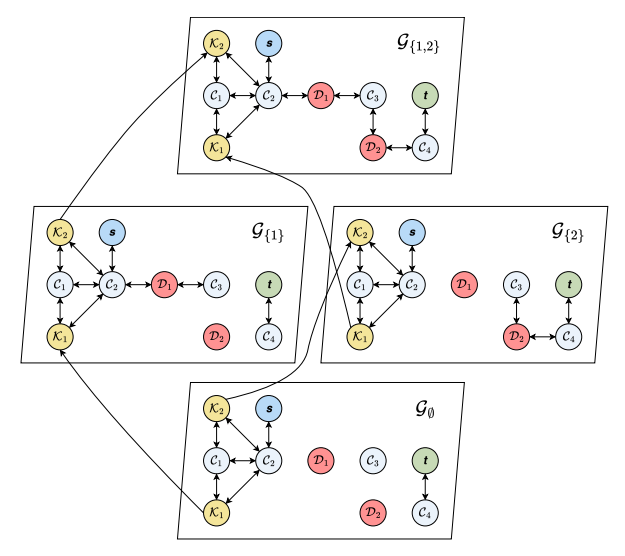


Fig. 3: The augmented GCS for a simple 2-key environment. The start point is located in free space node  $C_2$  and the target node is located in  $C_4$ .

start node in the base graph  $\mathcal{G}_{\emptyset}$ . Let  $S_1 \subset 2^{\mathcal{K}}$  denote the set of 1-element key sets, and let  $k_1 = |S_1|$ . The reachable keys can be found using breadth- or depth-first search on the base graph  $\mathcal{G}_{\emptyset}$ . For each key subset  $S \in S_1$ , we create a subgraph  $\mathcal{G}_S(\mathcal{V}_S, \mathcal{E}_S)$ . The vertex subset  $\mathcal{V}_S$  has a copy of all vertices in  $\mathcal{V}$ . The edge set is

$$\mathcal{E}_S = \mathcal{E}_\emptyset \cup \{(u, v) \in \mathcal{E} \mid u \in \mathbf{D}(S) \text{ or } v \in \mathbf{D}(S)\},\$$

which reinserts edges adjacent to the door corresponding to the key in S, denoted by  $\mathbf{D}(S)$ . We also add a directed edge to each reachable key node copy in  $\mathcal{V}_S$  from the corresponding key node copy in  $V_\emptyset$ . Since the key sets in configuration space associated with each key node copy are identical, these directed edges incur zero cost. (Alternatively, the corresponding key nodes in  $\mathcal{V}_S$  and  $\mathcal{V}_\emptyset$  can be *merged* into a single node.)

In our running 2-key example, both keys are reachable from the start node, so  $S_1 = \{\{1\}, \{2\}\}$  and  $k_1 = 2$ . The subgraphs  $G_{\{1\}}$  and  $G_{\{2\}}$  are shown in the middle of Fig. 3, along with the directed edges from key nodes in  $G_{\emptyset}$ .

**Layer 2.** The next layer corresponds to all 2-element key sets that are reachable from each of the 1-element key sets

in Layer 1. Let  $S_2 \subset 2^{\mathcal{K}}$  denote the set of 2-element key sets, and let  $k_2 = |S_2|$ . The 2-element reachable keys sets can again be found using breadth- or depth-first search within each subgraph from layer 1. As in layer 1, for each key subset  $S \in S_2$ , we create a subgraph  $\mathcal{G}_S(\mathcal{V}_S, \mathcal{E}_S)$  with vertex set  $\mathcal{V}_S$  featuring a copy of each vertex in  $\mathcal{V}$  and edge set given by

$$\mathcal{E}_S = \mathcal{E}_\emptyset \cup \{(u, v) \in \mathcal{E} \mid u \in \mathbf{D}(S) \text{ or } v \in \mathbf{D}(S)\},\$$

which reinserts edges adjacent to the doors corresponding to the keys in S, denoted by  $\mathbf{D}(S)$ . For each subgraph  $\mathcal{G}_S(\mathcal{V}_S,\mathcal{E}_S)$  and for each key node  $v\in\mathcal{V}_S$ , we add directed edges from the copy of key in subgraph  $\mathcal{G}_{S-\{v\}}$  in the previous layer.

In our running 2-key example, the only 2-element key set is the full key set, so  $S_2 = \{\{1,2\}\}$  and  $k_2 = 1$ . The subgraph  $G_{\{1,2\}}$  is shown at the top of Fig. 3.

**Layer**  $\ell$ . In general, layer  $\ell$  consists of subgraphs corresponding to all  $\ell$ -element key sets that are possible to reach from the starting node. Let  $S_{\ell}$  denote the set of  $\ell$ -element key sets. The reachable key sets are found by applying breadthor depth-first search from each subgraph at the previous layer. For each key subset  $S \in S_{\ell}$ , we create a subgraph  $\mathcal{G}_S(\mathcal{V}_S, \mathcal{E}_S)$  with vertex set  $\mathcal{V}_S$  featuring a copy of each vertex in  $\mathcal{V}$  and edge set given by

$$\mathcal{E}_S = \mathcal{E}_\emptyset \cup \{(u, v) \in \mathcal{E} \mid u \in \mathbf{D}(S) \text{ or } v \in \mathbf{D}(S)\},\$$

which reinserts edges adjacent to the doors corresponding to the keys in S. For each subgraph  $\mathcal{G}_S(\mathcal{V}_S, \mathcal{E}_S)$  and for each key node  $v \in \mathcal{V}_S$ , we add directed edges from the copy of key in subgraph  $\mathcal{G}_{S-\{v\}}$  in the previous layer.

**Layer**  $n_K$ . The final layer corresponds to the full key set  $\mathcal{K} \in 2^{\mathcal{K}}$  and consists of a single subgraph. The final graph  $\mathcal{G}_{\mathcal{K}}(\mathcal{V}_{\mathcal{K}}, \mathcal{E}_{\mathcal{K}})$  again has a vertex set  $\mathcal{V}_{\mathcal{K}}$  with a copy of each vertex in  $\mathcal{V}$  and has edge set  $\mathcal{E}_{\mathcal{K}} = \mathcal{E}$ , the same edge set as  $\mathcal{G}$ . For each key node  $v \in \mathcal{V}_{\mathcal{K}}$ , we add a directed edge from the corresponding key node in the graph  $\mathcal{G}_{\mathcal{K}-\{v\}}$ .

Finally, given a target node  $t \in \mathcal{V}_{\mathcal{C}}$  whose corresponding set contains the terminal condition, we merge all copies of the target node throughout all layers and subgraphs into a single node that serves as the target node in the augmented GCS. The algorithm for constructing the augmented graph is summarized in Algorithm 2.

For each subgraph in the augmented graph, we associate the free space partition sets, key sets, and door sets with the corresponding copies of the nodes to obtain the augmented GCS. The machinery of the GCS motion planning framework [4], [3] can now be applied to compute a shortest path from the start node to the (merged) target node in the augmented GCS. We now discuss the properties of these reformulations for the augmented GCS.

1) Properties of the augmented GCS: By construction, every path in the augmented GCS from the start node to the (merged) target node satisfies the key-door precedence logic. Therefore, a shortest path in the augmented GCS corresponds to an optimal solution of the original problem (1). The mixed-integer convex reformulation of the augmented GCS

### Algorithm 2: Augmented GCS Construction

```
Input: Labeled graph \mathcal{G}(\mathcal{V}, \mathcal{E}), with \mathcal{V} = {\mathcal{V}_{\mathcal{C}}, \mathcal{V}_{\mathcal{D}}, \mathcal{V}_{\mathcal{K}}},
        start node s \in \mathcal{V}_{\mathcal{C}}, target node t \in \mathcal{V}_{\mathcal{C}}
Output: Augmented graph \hat{\mathcal{G}}(\hat{\mathcal{V}}, \hat{\mathcal{E}})
   1: Create subgraph \mathcal{G}_{\emptyset}(\mathcal{V}_{\emptyset}, \mathcal{E}_{\emptyset}), where \mathcal{V}_{\emptyset} := \mathcal{V},
        \mathcal{E}_{\emptyset} := \mathcal{E} - \{(u, v) \in \mathcal{E} \mid u \in \mathcal{V}_{\mathcal{D}} \text{ or } v \in \mathcal{V}_{\mathcal{D}}\}
   2: for \ell = 1 to n_K do
             Find all reachable \ell-element key sets S_{\ell} \subset 2^{\mathcal{K}} from
             start node copy in all subgraphs with (\ell-1)-element
             key sets
             for S \in S_{\ell} do
   4:
                  Create subgraph \mathcal{G}_S(\mathcal{V}_S, \mathcal{E}_S), where \mathcal{V}_S := \mathcal{V},
   5:
                  \mathcal{E}_S := \mathcal{E}_{\emptyset} \cup \{(u, v) \in \mathcal{E} \mid u \in \mathbf{D}(S) \text{ or } v \in \mathbf{D}(S)\}
   6:
                        Add directed edge \mathcal{E}_S \leftarrow \mathcal{E}_S \cup \{(u,v)\}, where u
   7:
                        is the copy of v in \mathcal{V}_{S-\{v\}}
                  end for
   8:
             end for
   9:
 10: end for
 11: Merge copies of target node in all layers & subgraphs
12: return \hat{\mathcal{G}}(\hat{\mathcal{V}}, \hat{\mathcal{E}}), where \hat{\mathcal{V}} = \bigcup_{S \in \{S_{\ell}\}_{\ell=0}^{n_K}} \mathcal{V}_S,
        \hat{\mathcal{E}} = \cup_{S \in \{S_\ell\}_{\ell=0}^{n_K}} \mathcal{E}_S
```

based on [3], [4] thus exactly solves (1), up to a finite parameterization of the trajectory q (e.g., using Bézier curves). It is guaranteed to find a path if one exists (in the absence of a bound on the horizon T), and certifies infeasibility if a path does not exist. Infeasibility is certified if the (merged) target node is disconnected from the start node in the augmented graph.

A convex relaxation of the exact mixed-integer formulation, obtained by simply dropping binary constraints, along with an inexpensive rounding scheme, can be used to obtain approximate solutions to (1). It was observed in [4] that in many practical motion planning problems (without precedence specifications), this relaxation is often tight and provides certifiably near-optimal solutions. We will study the tightness of this relaxation for problems with precedence specifications in our numerical experiments in the next section.

Further, even the convex relaxation can be challenging to solve in practice. It may be computationally expensive to find an exact convex partition from Section III with the minimum number of free space nodes. Also, the infinite-dimensional trajectory q is discretized with Bézier curves of finite order.

2) Size of the augmented GCS: The number of subgraphs in the augmented GCS depends on the number of reachable key sets. Let us obtain an upper bound on the number of subgraphs in the augmented GCS. For an environment with  $n_K$  keys and associated doors, recall that  $S_k \in 2^K$  denotes the set of reachable k-element key subsets, each of which corresponds to a subgraph in the augmented GCS. The total number of subgraphs satisfies

$$\sum_{k=0}^{n_K} |S_k| \le \sum_{k=0}^{n_K} \binom{n_K}{k} = 2^{n_K}. \tag{4}$$

To see this, at the kth layer in the augmented graph, there are at most  $\binom{n_K}{k}$  possible reachable key subsets. The bound is obtained when every key is reachable from the starting node. Thus, in the worst case, the total number of subgraphs is exponential in the number of keys.

For a lower bound on the number of subgraphs in the augmented graph, note that there are degenerate cases where some keys are not reachable from the start node. For example, if none of the keys are reachable from the start node, there is only a single copy of the labeled graph in the augmented graph, and the problem reduces to a shortest path problem on the original graph. When only a single additional key is reachable at each layer (i.e., the  $S_k$  each contain only one element, meaning that the keys must be obtained in a specific sequence), then there are only  $n_K+1$  subgraphs in the augmented graph. In many practical problems, there are a small number of keys, and the augmented graph has limited width. Fig. 4 shows the graphs of subgraphs for up to 4 keys when all key subsets are reachable.

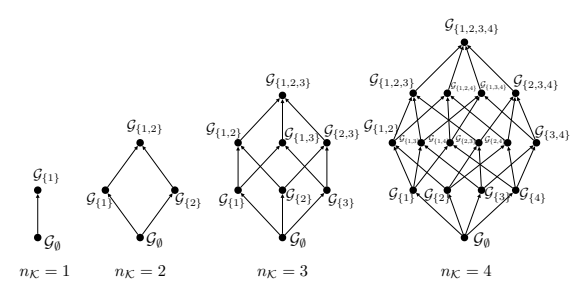


Fig. 4: Figure illustrating the size of the augmented GCS through graphs of subgraphs up to  $n_K = 4$  keys.

### V. NUMERICAL EXPERIMENTS AND KEY-DOOR MAZE GENERATOR

In this section, we demonstrate and evaluate the proposed approach to solving a variety of key-door environments. Two benchmarks from [5] are shown in Sections V.A. Then we present a method to generate benchmark mazes with keys and doors and present numerical experiments on instances created with this benchmark generator. Code for reproducing these results will be provided in an open-source repository. All experiments were performed on a laptop with an Apple M2 CPU and 8GB RAM. The underlying convex optimization solver was MOSEK [12], accessed via the GCS components from the Drake [13] Python bindings. The source code and numerical results are publicly available at https://github.com/TSummersLab/gcspy-precedence-specifications.

### A. Key-Door Environments from [5]

**2-Key Environment.** We first consider the simple keydoor environment with two keys and two doors shown in Fig. 2. The robot must pick up two keys to open two doors in order to reach the target set, which can be written as the STL formula  $\varphi = \mathcal{K}_1 \mathcal{R} \neg \mathcal{D}_1 \wedge \mathcal{K}_2 \mathcal{R} \neg \mathcal{D}_2 \wedge \mathcal{F} \mathcal{T}$  (which in this case is equivalent to the formula  $\neg \mathcal{D}_1 \mathcal{U} \mathcal{K}_1 \wedge \neg \mathcal{D}_2 \mathcal{U} \mathcal{K}_2 \wedge \mathcal{F} \mathcal{T}$ ).

We used Algorithm 1 to create an exact convex partition and labeled GCS. Next we used Algorithm 2 to construct the augmented GCS, shown in Fig. 3. Then we used the GCS components in Drake [13] and the optimization solver Mosek [12] to solve a shortest path problem for the augmented GCS. The augmented GCS construction time is **0.0108** seconds and the solving time is **0.249** seconds. Compared with an approach that uses general-purpose temporal logic tools [5], our augmented GCS construction is about 80x faster.

**5-Key Environment.** We also solved a 5 key-door environment from [5]. The STL formula can be written as

$$\varphi = \mathcal{K}_1 \mathcal{R} \neg \mathcal{D}_1 \wedge \mathcal{K}_2 \mathcal{R} \neg \mathcal{D}_2 \wedge \mathcal{K}_3 \mathcal{R} \neg \mathcal{D}_3$$
$$\wedge \mathcal{K}_4 \mathcal{R} \neg \mathcal{D}_4 \wedge \mathcal{K}_5 \mathcal{R} \neg \mathcal{D}_5 \wedge \mathcal{F} \mathcal{T}.$$
 (5)

The exact convex partitioning from Algorithm 1 produces a graph with 25 free space cells, 5 key cells, 5 door cells. The augmented GCS constructed by Algorithm 2 contains six layers with nine subgraphs. The augmented GCS construction time is **0.0423** seconds and the solving time is **1.573** seconds. Compared with an approach that uses general-purpose temporal logic tools [5], our augmented GCS construction is more than 50000x faster, and our solve time is about 3.5x faster.

### B. Key-Door Maze Benchmark Generator

To quickly generate multiple instances of maps with doors and keys to test the algorithm, a maze benchmark generator was created. The generator creates key-door mazes in three steps. First, a perfect maze is generated using Eller's algorithm [14]. A perfect maze has a tree structure, where there is a unique path between any two cells in the maze. Second, the start and target cells are assigned randomly, and doors and keys are placed based on a series of breadthfirst searches (described in more detail below). All mazes are feasible by construction and have the same number of keys and doors. Third, optionally, walls can be added and/or removed randomly to adjust the width of the associated augmented graph and potentially create infeasibility. This step makes the mazes imperfect since the removal of walls creates branching paths and loops through the environment, making them more challenging to solve. Example mazes are shown in Fig. 5.

Finally, a graph of convex sets is created to represent connectivity among free space, key, and door cells.

**Maze Generator.** Eller's algorithm rapidly generates a perfect maze one row at a time [14]. It is faster and more memory efficient than alternative maze generation algorithms such as recursive backtracking because it works with at most two rows at once. The number of rows and columns is required to be odd. For any natural numbers r and c, a maze is created with 2r+1 rows and 2c+1 columns. The starting cell is then randomly selected to be in the center or in one of the corners. The target cell is selected to be the cell farthest from the starting cell based on a breadth-first search.

**Key-Door Batches.** To create a variety of augmented GCS structures, doors and keys are placed in *batches*. A batch is an integer composition of the total number of key-door

pairs and represents how many keys will be accessible either at the start or after a certain number of doors has been unlocked. For example, with 10 key-door pairs, the batch (1,1,2,1,1,1,1,2) creates a narrow maze, with only 1 or 2 keys accessible after opening any door, and the batch (4,6) creates a wide maze, with 4 keys accessible from the start and 6 keys accessible after opening the first 4 doors, respectively. An example of a narrow maze and a wide maze can be seen in Fig. 5.

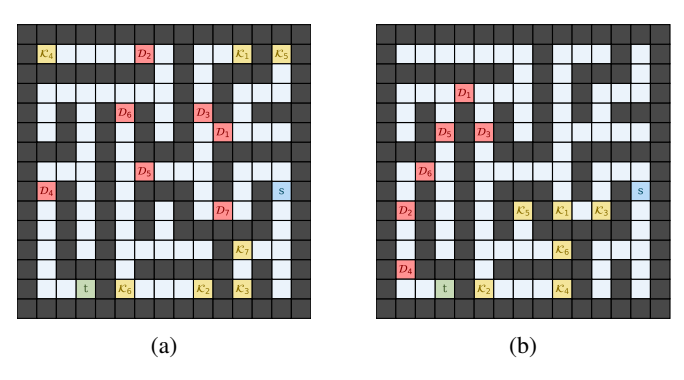


Fig. 5: Example mazes: (a) narrow maze with key-door batch (1, 2, 1, 1, 2), (b) wide maze with key-door batch (7).

**Door Placement.** For each batch the doors are placed first then the keys. The doors are placed along a path that starts at a target cell and ends at the start cell. For the first batch, the goal cell is the same as the target cell and for the rest of the batches the goal cell is the closest key to the start. The doors are placed in hallways, never in intersections or corners. The larger the batch the closer each door will be relative to each other and the smaller the batch the more spread out each door will be. If the path between the last door is too short or the door is too close to the start it will not be placed. This allows room for the keys to be placed. In the case where the number of doors placed is less than the current batch size, the current batch size will be reduced to equal the number of doors.

**Key Placement.** After at least one door has been placed, the keys are placed. The first key is placed in the furthest cell from the start. If the current batch is larger than 1, sequential keys are placed in the dead ends and corners near this key. If the current batch is larger than 1 and the number of keys is less than the number of doors, then one door is removed. Another attempt is then made to place the same number of keys as doors. This process continues until the number of keys is the same as the number of doors. For example, if the number of doors placed is 5 but only 3 keys were placed one door is removed and it attempts to place 4 keys. If only 3 keys could be placed then one more door is removed and it again attempts to place 3 keys. This converts the current batch from 5 to 3. In the case where no keys can be placed and one door remains then that door is removed. After one batch is complete the next one begins in a similar process except the new goal cell becomes the closet key to the start. If no keys are placed the remaining batches, if any, are skipped.

Removing or Adding Walls. Once keys and doors have been placed, the maze can be modified by removing a

ID	$ \mathcal{V} $	$ \hat{\mathcal{V}} $	# of keys	Max width	Form GCS (s)	Solve (s)	$\delta_{relax}$ (%)
1	21	114	2	1	0.00585	0.0408	0
2	23	160	3	1	0.00777	0.0536	0
3	74	974	5	2	0.0321	0.274	0
4	78	3808	5	7	0.137	3.87	0.947
5	82	5728	5	10	0.214	4.53	0.363
6	273	5786	10	1	0.174	1.46	0
7	274	11480	10	3	0.4	25.5	0.744
8	284	56976	10	16	2.11	545	0.126
9	1468	11720	3	1	0.347	3.98	0

TABLE I: Numerical Experiments with Key-Door Mazes

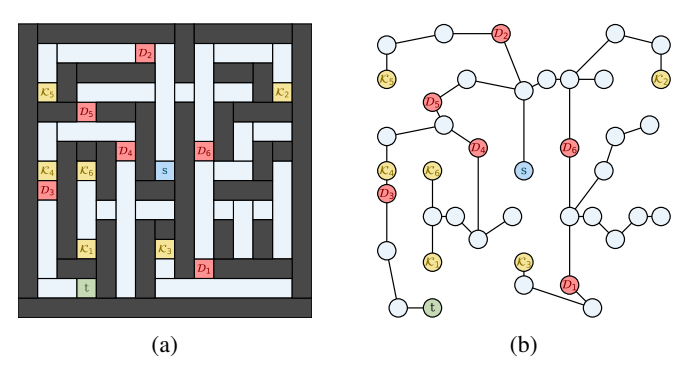


Fig. 6: (a) key-door maze, (b) graph of maze.

random set of walls. Candidate walls for removal are those not on the border, next to a door, or a corner. Each candidate wall is removed with a specified probability, which is a parameter in the code. Removing walls has the effect of widening the associated augmented graph by increasing the number of accessible keys at each layer. It may also make some or even all keys unnecessary. Additionally, the maze can be altered and potentially made infeasible by randomly adding a wall in a hallway, which may block access to a door, key, or the goal.

**Graph Creation and Cell Merging.** Since the cells are arranged in a grid, it is easy to construct a connectivity graph of the free space, key, and doors cells, so we do not use Algorithm 1 for partitioning. Further, adjacent cells are merged to reduce the number of nodes in the graph. Free space cells are first merged horizontally, then vertically. The vertex representations for the merged free space cells, and for key and door cells are stored. After merging, cell vertices are stored with labels 's', 't', 'd#', 'k#', or 'c#' for start, target, door, key, or cell, along with an edge list. Fig. 6 shows the graph representation of a partitioned and merged maze.

### C. Numerical Experiments on Key-Door Mazes

We evaluate the performance of the proposed approach on a set of key-door mazes created by the our generator. For each maze, we used Algorithm 2 to construct the augmented GCS and then used the GCS components in Drake [13] and the optimization solver Mosek [12] to solve a shortest path problem for the augmented GCS. In particular, we solve a convex relaxation of the exact mixed-integer convex reformulation and obtain a suboptimal solution via a rounding scheme, as described in [4], [3]. Table I shows

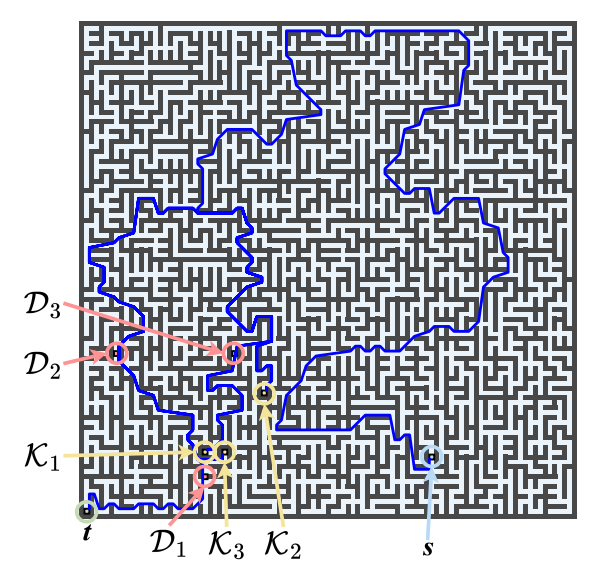


Fig. 7: A 99×99 maze with 3 keys and 3 doors.

the results of nine experiments. For each experiment, we report the number of vertices in the base GCS,  $|\mathcal{V}|$ ; the number of vertices in the augmented GCS,  $|\hat{\mathcal{V}}|$ ; the number of keys; the maximum number of subgraphs in any layer of the augmented GCS, which we call the max width; the augmented GCS construction time; the augmented GCS solving time; and an upper bound on the optimality gap, given by

$$\delta_{relax} = \frac{C_{round} - C_{relax}}{C_{relax}},$$

where  $C_{relax}$  is the cost of the relaxation, which lower bounds the optimal value, and  $C_{round}$  is the cost of the rounded solution.

**Discussion.** We make several observations based on the results in Table I. First, our approach scales to much larger problems than reported in [5]. In experiment 6, we solve a maze with 10 keys within 2 seconds. In experiment 9, we solve a large maze with 3 keys within 4 seconds, where the base GCS with 1468 vertices and the augmented GCS has 11720 vertices. The solution is shown in Fig. 7. In all instances the rounded solution is within 1% of the global optimum, and in most cases is certified as globally optimal.

The max width has a significant effect on the size of the augmented GCS and the solve time. Experiment 8 has 10 keys and a max width of 16, yielding an augmented GCS with 56976 vertices and a solve time of 545 seconds. Further, the instances with non-zero optimality gap are the wider

mazes with more possible orders in which to pick up keys. Scaling to environments with many keys and large width will likely require heuristics that trade off computation time with solution quality, which will be explored in future work.

#### REFERENCES

- S. M. LaValle, *Planning algorithms*. Cambridge University Press, 2006
- [2] J.-C. Latombe, Robot motion planning. Springer Science & Business Media, 2012.
- [3] T. Marcucci, J. Umenberger, P. Parrilo, and R. Tedrake, "Shortest paths in graphs of convex sets," *SIAM Journal on Optimization*, 2024.
- [4] T. Marcucci, M. Petersen, D. von Wrangel, and R. Tedrake, "Motion planning around obstacles with convex optimization," *Science robotics*, 2023.
- [5] V. Kurtz and H. Lin, "Temporal logic motion planning with convex optimization via graphs of convex sets," *IEEE Transactions on Robotics*, 2023.
- [6] C. R. Garrett, R. Chitnis, R. Holladay, B. Kim, T. Silver, L. P. Kaelbling, and T. Lozano-Pérez, "Integrated task and motion planning," *Annual review of control, robotics, and autonomous systems*, 2021.
- [7] O. Maler and D. Nickovic, "Monitoring temporal properties of continuous signals," in *International symposium on formal techniques in real-time and fault-tolerant systems*. Springer, 2004.
- [8] C. Baier and J.-P. Katoen, Principles of model checking. MIT press, 2008
- [9] D. Avis and K. Fukuda, "Reverse search for enumeration," Discrete applied mathematics, 1996.
- [10] J. Shaikh, D. Gostin, and J. P. Koeln, "Exact obstacle-free space representation using hybrid zonotopes," in 2025 American Control Conference, 2025.
- [11] T. Geyer, F. D. Torrisi, and M. Morari, "Optimal complexity reduction of polyhedral piecewise affine systems," *Automatica*, 2008.
- [12] MOSEK, The MOSEK Python Fusion API manual. Version 11.0., 2025. [Online]. Available: https://docs.mosek.com/latest/pythonfusion/index.html
- [13] R. Tedrake and the Drake Development Team, "Drake: Model-based design and verification for robotics," 2019. [Online]. Available: https://drake.mit.edu
- [14] J. Buck, Mazes for Programmers: Code Your Own Twisty Little Passages. Pragmatic Bookshelf, 2015.